A Local Mobility Model for Ultra-Thin DGSOI nMOSFETs

Andreas Schenk

Integrated Systems Lab., ETH Zürich, Gloriastr. 35, CH-8092 Zürich, Switzerland
schenk@iis.ee.ethz.ch

Abstract

The derivation of a local mobility model for symmetrical ultra-thin DGSOI nMOSFETs is outlined. A local-field variant is found to reproduce the dependencies of the quantum-mechanical mobility on silicon slab thickness and normal field with a maximum error of 10%. The model can be used with the density-gradient approach.

1 Introduction

Currently there is strong interest in ultra-thin DGSOI transistors due to their potential perspectives for better scalability, higher performance, and reduced short-channel effects. A theoretical enhancement of the low-field mobility for silicon slab thicknesses $t_{\mathrm{Si}} \approx 10\,\mathrm{nm}$ was shown to be unique to *symmetrical* variants [1]. TCAD application with DESSIS$_{-\mathrm{ISE}}$ of an integrated quantum-mechanical (q.m.) mobility model based on a 1D Schrödinger/Poisson solver was demonstrated in [1, 2]. However, limited numerical robustness and considerable CPU times call for a simple local model. Whereas local mobility models for single-gate MOSFETs [3, 4] are widely used in the TCAD community, a similar model for ultra-thin DGSOI devices is still missing. The aim of this paper is to outline the derivation of such a model, to point out the particular difficulties involved, and to discuss its accuracy compared to the q.m. model.

2 Model Restrictions and Development Strategy

The complex physics and the dependence on various parameters require a step-by-step development of such a model. In a first step which is outlined in this paper we neglect all kinds of Coulomb scattering [5] and restrict ourselves to symmetrical DGSOI nMOSFETs. We assume equal roughness of both interfaces with parameters that reproduce the measured universal $\mu_{\mathrm{eff}}(E_{\mathrm{eff}})$ dependence of bulk MOSFETs [6] ($\Delta_{1,2} = 0.32\,\mathrm{nm}$, $L_{1,2} = 1.5\,\mathrm{nm}$). Electron-phonon coupling constants and effective phonon energies are assumed to keep their bulk values even for the thinnest silicon slabs. We neglect poly-silicon effects (i.e. actually assume metal-gate boundary conditions) and also disregard longitudinal quantum effects ($L_{\mathrm{G}} \geq 20\,\mathrm{nm}$). Nonparabolicity ($\alpha = 0.5/\,\mathrm{eV}$) is included, because it has a 10% effect on the mobility. It turns out that the effective mobility only weakly depends on the oxide thickness t_{ox}. Therefore, we omit this dependence in a first step and use $t_{\mathrm{ox}} = 0.6\,\mathrm{nm}$ throughout the simulations. The subsequent inclusion of this dependence in one parameter of the local model would be straightforward. From the simulated $\mu_{\mathrm{eff}}(E_{\mathrm{eff}})$ curves in the t_{Si}-range from 1 nm to 15 nm (Fig. 1) we extract the low-field parameter $\mu_{\mathrm{low}}(t_{\mathrm{Si}})$ as function of silicon slab thickness. This dependence is shown on the right-hand side of Fig. 1. One observes

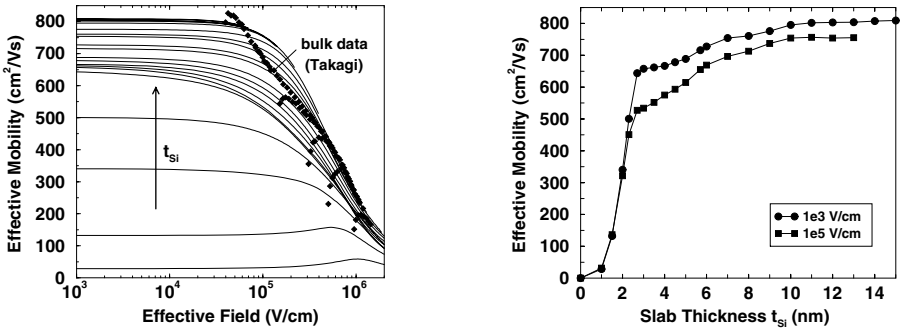

Figure 1: Left: Effective mobility as function of effective field $E_{\rm eff}$ for Si slab thicknesses $t_{\rm Si}$ in the range from 1 nm to 15 nm (no Coulomb scattering). The values of $t_{\rm Si}$ are listed in Table 1. Right: Effective mobility versus slab thickness $t_{\rm Si}$ for two values of the effective field. A cubic-spline fit to the upper curve yields the parameter $\mu_{\rm low}(t_{\rm Si})$ for the local model.

$t_{\rm Si}$ (nm)	1.0	1.5	2.0	2.3	2.7	3.0	3.5
$\mu_{\rm low}$ (cm^2/Vs)	28.81	132.5	340.65	500.44	643.51	657.29	661.92
$t_{\rm Si}$ (nm)	4.0	4.5	5.0	5.7	6.0	7.0	8.0
$\mu_{\rm low}$ (cm^2/Vs)	666.5	678.3	688.29	715.6	727.37	753.75	760.81
$t_{\rm Si}$ (nm)	9.0	10	11	12	13	14	15
$\mu_{\rm low}$ (cm^2/Vs)	775.98	795.3	801.81	803.30	803.6	807.13	809.21

Table 1: Low-field values of $\mu_{\rm eff}(t_{\rm Si})$ from which the cubic-spline function $\mu_{\rm low}(t_{\rm Si})$ can be generated.

the region of geometrical confinement ($t_{\rm Si} < 3$ nm) with a rapid decay of the mobility and a broad maximum around $t_{\rm Si} \approx 10$ nm, where the mobility is enhanced by 10% – 15% in virtue of interference between the two channels. The remaining structure around $t_{\rm Si} \approx 7$ nm is real (mesh-refinement effects are much smaller). For the parameterization of this involved $\mu_{\rm low}(t_{\rm Si})$-dependence any analytical ansatz fails; therefore a cubic-spline interpolation based on the discrete data points is the best alternative. This spline can be generated from Table 1. The $\mu_{\rm eff}(E_{\rm eff})$-dependence with its $t_{\rm Si}$-independent high-field limit for $t_{\rm Si}$ >5 nm (Fig. 1) suggests a simple local model of the form $\mu(E_\perp, t_{\rm Si}) = \mu_{\rm low}(t_{\rm Si})/(1 + (E_\perp/E_{\rm ref})^{b_E})$ with two $t_{\rm Si}$-dependent parameters $E_{\rm ref}$ and b_E. In order to find a suitable parameterization of these functions, the only promising way is to use $\mu_{\rm eff}(E_{\rm eff})$ instead of some $\mu_{\rm loc}(E_{\perp,\rm loc})$ from an inner point, e.g. at the surface. Therefore, the functions $E_{\rm ref}(t_{\rm Si})$ and $b_E(t_{\rm Si})$ are determined iteratively by non-linear curve fitting to each curve on the left-hand side of Fig. 1. As a result, $E_{\rm ref}(t_{\rm Si})$ and $b_E(t_{\rm Si})$ become available in form of algebraic expressions.

3 Local-Field versus Local-Density Model

If the parameterization obtained in this way is applied to the local-field model, a larger error must be expected for the on-current. Since the $E_\perp$-field in the center is always zero, the local mobility will be pinned to its low-field value there, whereas the q.m. mobility drops with increasing gate voltage (right-hand side of Fig. 2). The charge density, on the other hand, has a substantial value in the center of ultra-thin DGSOIs. The resulting error for the on-current can be seen from the left-hand side of Fig. 2. To

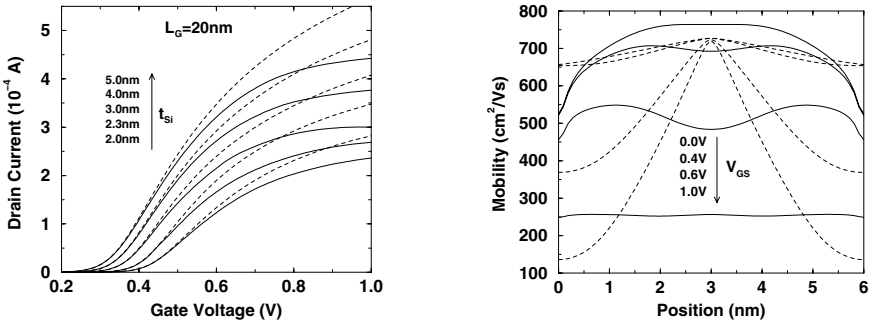

Figure 2: Left: Transfer characteristics at $V_{\rm DS} = 10\,$mV for $2\,{\rm nm} \leq t_{\rm Si} \leq 6\,$nm. Right: Evolution (from top to bottom) of the mobility profiles across the slab with increasing $V_{\rm GS}$ in the case of $t_{\rm Si}$ = 6 nm. Solid lines: q.m. model, dashed lines: local-field model.

overcome this problem, a parameterization of the mobility in terms of the density was taken into consideration. The resulting local-density model $\mu(n, t_{\rm Si}) = \mu_{\rm low}(t_{\rm Si})/(1 + (n/n_{\rm ref})^{b_n})$ with the local 3D density n was developed on the same lines as the local-field model. Starting point were the simulated functions $\mu_{\rm eff}(n_{\rm av})$ for the same $t_{\rm Si}$-range as in Fig. 1. Iterative non-linear curve fitting yielded the two parameters $n_{\rm ref}(t_{\rm Si})$ and $b_n(t_{\rm Si})$. The mobility profiles of the local-density model have minima exactly where the density has its maxima (immediately obvious from the formula of the local-density model). This results in an underestimation of the on-current with an amount

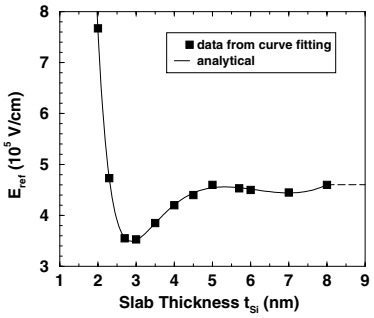

c_0	-6.24142 e6	c_{-4}	-8.01531 e7
c_{-1}	3.5754 e7	c_1	9.49686 e5
c_{-2}	-1.14565 e8	c_2	-9.62632 e4
c_{-3}	1.69859 e8	c_3	4.44057 e3

Figure 3: Final fit of the function $E_{\rm ref}(t_{\rm Si})$ (solid line) with coefficients c_n given in the table.

which is even stronger than the overestimation by the local-field model. For the purpose of a TCAD model, transfer characteristics at $V_{\rm DS} = 10\,$mV were then used in order to re-adjust the parameters $E_{\rm ref}(t_{\rm Si})$ and $b_E(t_{\rm Si})$ for a close fit to the currents. The $t_{\rm Si}$-dependence of these parameters greatly simplifies ($b_E(t_{\rm Si})$ can be taken as a constant 1.7) and the maximum relative error becomes 10% for $t_{\rm Si} > 2\,$nm (Fig. 4). The final model reads

$$\mu(E_\perp, t_{\rm Si}) = \frac{\mu_{\rm low}(t_{\rm Si})}{1 + \left[E_\perp / E_{\rm ref}(t_{\rm Si})\right]^{1.7}} \quad \text{with}$$

$$E_{\rm ref}(d) = C(d)\,\Theta(8-d) + C(8)\,\Theta(d-8), \qquad C(d) = \sum_{n=-4}^{+3} c_n\, d^n$$

where $d = t_{\rm Si}/nm$. The coefficients c_n are given in the table of Fig. 3.

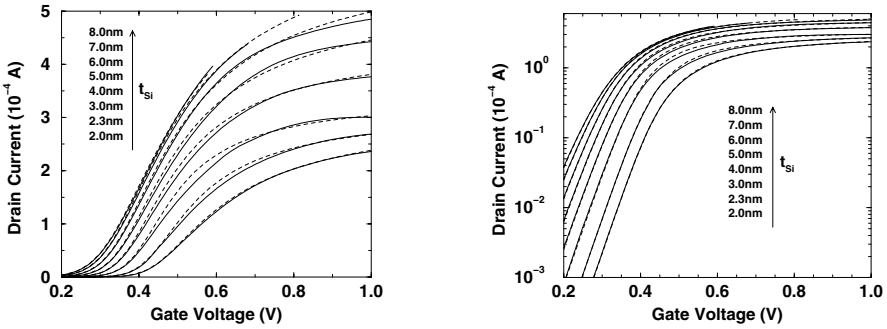

Figure 4: Transfer characteristics at $V_{\mathrm{DS}} = 10\,\mathrm{mV}$ for $2\,\mathrm{nm} \leq t_{\mathrm{Si}} \leq 8\,\mathrm{nm}$ with the q.m. model (solid lines) and the final local-field model (dashed lines). Left: lin-lin scale, right: lin-log scale.

4 Conclusion

A local-field model for the mobility of symmetrical ultra-thin DGSOI nMOSFETs is demonstrated to reproduce transfer characteristics with a maximum error of 10% for silicon slab thicknesses $t_{\mathrm{Si}} > 2\,\mathrm{nm}$. The accuracy is limited by the general impossibility to map a nonlocal q.m. quantity to the corresponding local classical quantity. As in the case of established local mobility models for single-gate transistors, the usability of the presented model comes from the crossing of q.m. and local mobility profiles at points of high electron and current densities. In single-gate transistors these points coincide with the single centroids of the relatively sharp density distributions. In ultra-thin DGSOI devices volume inversion leads to a high density in the middle of the silicon slab, too, which makes the method less straightforward. Besides negligible CPU time the actual advantage of the local model is that a Schrödinger-Poisson solver becomes dispensable, because only the q.m. normal field is needed. The latter can already be obtained by the density-gradient approach.

Acknowledgment

The author is grateful for many valuable discussions with Dr. A. Wettstein (ISE AG Zurich) and for the financial support by Fujitsu Laboratories Ltd.

References

[1] A. Schenk and A. Wettstein, "Simulation of DGSOI MOSFETs with a Schrödinger-Poisson Based Mobility Model", Proc. SISPAD 2002, pp. 21–24.

[2] A. Wettstein, "Quantum Effects in MOS Devices", PhD Thesis No. 13649, ETH Zrich, ISBN: 3-89649-566-6, Hartung-Gorre, 2000.

[3] S. A. Schwarz and S. E. Russek, "Semi-Empirical Equations for Electron Velocity in Silicon", IEEE Trans. El. Dev., ED-30 (12), pp. 1629–1633, 1983.

[4] M. N. Darwish, J. L. Lentz, M. R. Pinto, P. M. Zeitzoff, T. J. Krutsick, and H. H. Vuong, "An Improved Electron and Hole Mobility Model for General Purpose Device Simulation", IEEE Trans. El. Dev., ED-44 (9), pp. 1529–1537, 1997.

[5] F. Gamiz and M. V. Fischetti, "Remote Coulomb Scattering in MOSFETs: Screening by Electrons in the Gate", APL 83 (23), pp. 4848–4850, (2003).

[6] S. Takagi, A. Toriumi, M. Iwase, and H. Tango, "On the Universality of Inversion Layer Mobility in Si MOSFET's", IEEE Trans. El. Dev., ED-41 (12), pp. 2357–2368, 1994.